

MoveOD: Synthesizing Origin-Destination Commute Distribution from U.S. Census Data

Rishav Sen

Electrical and Computer Engineering
Vanderbilt University
 Nashville, United States
 rishav.sen@vanderbilt.edu

Abhishek Dubey

Electrical and Computer Engineering
Vanderbilt University
 Nashville, United States
 abhishek.dubey@vanderbilt.edu

Ayan Mukhopadhyay

Computer Science
Vanderbilt University
 Nashville, United States
 ayan.mukhopadhyay@vanderbilt.edu

Samitha Samaranayake

Civil and Environmental Engineering
Cornell University
 Ithaca, United States
 samitha@cornell.edu

Aron Laszka

Computer Science
Pennsylvania State University
 State College, United States
 aql5923@psu.edu

Abstract—High-resolution origin-destination (OD) tables are essential for a wide spectrum of transportation applications, from modeling traffic and signal timing optimization to congestion pricing and vehicle routing. However, outside a handful of data rich cities, such data is rarely available. We introduce MOVEOD, an open-source pipeline that synthesizes public data into commuter OD flows with fine-grained spatial and temporal departure times for any county in the United States. MOVEOD combines five open data sources – American Community Survey (ACS) departure time and travel time distributions, Longitudinal Employer-Household Dynamics (LODES) residence-to-workplace flows, county geometries, road network information from OpenStreetMap (OSM), and building footprints from OSM and Microsoft, into a single OD dataset. We use a constrained sampling and integer-programming method to reconcile the OD dataset with data from ACS and LODES. Our approach involves: (1) matching commuter totals per origin zone, (2) aligning workplace destinations with employment distributions, and (3) and calibrating travel durations to ACS-reported commute times. This ensures the OD data accurately reflects commuting patterns. We demonstrate the framework on Hamilton County, Tennessee, where we generate roughly 150,000 synthetic trips in minutes, which we feed into a benchmark suite of classical and learning-based vehicle-routing algorithms. The MOVEOD pipeline is an end-to-end automated system, enabling users to easily apply it across the United States by giving only a county and a year; and it can be adapted to other countries with comparable census datasets. The source code and a lightweight browser interface are publicly available.

Index Terms—Origin-Destination dataset, Urban Mobility, Transportation Planning, Travel Demand Modeling.

I. INTRODUCTION

Granular origin-destination (OD) travel demand data is a foundational component of traffic analysis, transit optimization, and urban infrastructure planning. Recent advances in machine learning have significantly expanded the use of such data across transportation [8], [24], [43]. In traffic engineering, OD datasets are essential for modeling traffic flow, optimizing signal timing, mitigating congestion, and

informing investments in new roadway or public infrastructure. Similarly, public transit agencies rely heavily on OD data [42], [44] to optimize fixed-route services, design flexible micro-transit solutions, and plan network expansions based on real travel patterns. Beyond infrastructure and operations, OD information supports accident analysis and proactive safety interventions, such as targeted signage improvements, road geometry adjustments, and intersection redesigns [16], [17].

However, collecting fine-grained, building-level origin-destination (OD) data remains a persistent challenge. Traditional methods, such as household travel surveys, Bluetooth MAC trackers, or mobile GPS traces are often sparse, noisy, or available only for specific travel modes. These sources struggle to generalize across urban, suburban, and rural environments which poses a significant challenge for the over 3000 smaller transit agencies across the United States that lack integrated data pipelines [32]. For example, New York City has rich taxi trip data [11], but this dataset captures only a single travel mode and misses the broader commuting population.

There are several publicly available nationwide datasets that capture some aspects of commuting; however, none of them provide a complete distribution: The American Community Survey (ACS) [30] and Longitudinal Employer-Household Dynamics (LODES) [1] provide aggregate counts of residents and jobs by census unit, but they lack departure times and fine-grained (i.e., building-level) locations. Building footprints from OpenStreetMap (OSM) [29] or Microsoft Building Footprints (MSBF) [15] pinpoint every structure, but they contain no occupancy or travel-demand information. Traffic datasets (e.g., INRIX) provide fine-grained information on traffic demand aggregated over road segments, but this cannot be decomposed into individual OD trips. Naïvely combining these marginal datasets (e.g., via iterative proportional fitting) may yield implausible results, such as hundreds of commuters

assigned to a small residential building or a remote facility with limited commuter access or every commuter departing in a single rush-hour spike. These limitations motivate a synthetic approach: generate statistically consistent OD data by reconciling multiple incomplete but complementary datasets. Although synthesis introduces challenges such as building a realistic joint distribution over origins, destinations, and times to match marginal distributions, it offers a scalable path to high-fidelity OD estimation for regions that lack ground-truth data.

In this work, we introduce MOVEOD, an open-source framework for synthesizing granular, time-dependent OD datasets by integrating several public data sources: ACS, LODES, OSM, and Microsoft Building Footprints and road speeds. Each source offers partial views, as discussed earlier. Importantly, while MOVEOD produces synthetic data, it maintains statistical fidelity to real-world patterns by matching observed marginals (residence-workplace locations, departure times, travel durations) while enforcing spatial coherence. This enables its use in evaluating machine learning models, policy interventions, and transit system designs.

We focus specifically on daily commuting trips between residences and workplaces, allowing MOVEOD to leverage spatial employment and housing density data while avoiding poorly measured recreational or freight travel. The resulting dataset is spatially granular, assigning trip origins and destinations to specific buildings, and temporally distributed, modeling departure time variability and travel durations using traffic data [20], [38].

Our core contribution is not a static dataset, but a modular synthesis approach: MOVEOD can generate OD datasets for any U.S. county and, in principle, for any region where similar marginal datasets are available, and we release an interactive, easy-to-use platform to generate commute OD data. To demonstrate its utility, we apply MOVEOD to Hamilton County and Davidson County in Tennessee, United States. We evaluate the synthetic OD dataset of Hamilton County on a downstream task involving vehicle routing optimization using state-of-the-art algorithms.

The rest of the paper is organized as follows: Section II reviews the literature on origin–destination estimation. Section III outlines the problem setup and data sources. Section IV describes the synthesis pipeline, and Section V explains the calibration procedure used to align the synthetic OD data with ACS commuter distributions. Section VI details the experimental setup, while Section VII presents benchmarking results using state-of-the-art vehicle routing algorithms. Finally, Section VIII discusses limitations and future opportunities.

II. RELATED WORKS

A. Open Benchmarks for Transportation AI

The past few years have witnessed remarkable growth in large-scale, openly licensed datasets that have catalyzed progress in traffic forecasting, routing, and autonomous driving research. Early sensor centric research such as METR-LA and PEMS-BAY [25] sparked the first wave of spatio-temporal

graph neural networks; subsequent releases expanded in size (e.g., LARGEST [26]) or semantic richness (e.g., SCENARIO NET [23]). While indispensable, these datasets share two limitations that are critical for OD research: (i) they focus on traffic states measured at fixed sensor locations, not on the population-level flows between origins and destinations; (ii) Coverage is typically confined to a few metropolitan areas, hindering work on domain transfer and equitable deployment across diverse cities.

B. Origin–Destination Estimation and Simulation

Traditionally, OD estimation has relied on household travel surveys [37] or gravity and friction-factor models calibrated with stationary counts [28]. Newer data sources such as mobile phone location tracking [18], Bluetooth location identification [5], and ride-hailing trip records [7] have improved temporal resolution, but these methods still tend to focus on large cities where such data is readily available. Several open projects attempt full synthetic generation. Open-PFLOW [19] uses stochastic methods to allocate commuting trips to census microdata, providing disaggregate, time-resolved movement data that enables analysis of flows at different times of day. However, its extensibility beyond Japan is limited, and the generation process can rely on private or commercial datasets for detailed spatial information, such as building locations and road networks. The vehicle-network simulator of [41] produces microscopic trajectories for Vehicular Ad Hoc Network (VANET) studies, yet its demand model is tuned to a single European city and lacks transparency in demographic assumptions.

C. Public-Transit and Multi-Modal Planning

Modern, data-driven transit planning uses OD matrices to size fleets and schedule services [2], [4]. Having finer-grained OD data improves the calibration of discrete-choice models [13] and supports more accurate multi-modal assignment [12]. However, most public transit simulations [27], [36] assume a fixed commuter OD table obtained from proprietary surveys, limiting reproducibility and flexibility across different agencies.

D. Advancing the State of the Art

MOVEOD fills a critical gap between sensor-centric traffic benchmarks and synthetic population measurement tools, supplying the first openly licensed, high-resolution commuter OD datasets for every U.S. county while providing a reproducible toolkit for future extensions. Compared to traditional survey-based methods or synthetic generators focused on a single city, MOVEOD offers three key improvements:

- 1) **Nationwide scalability.** MOVEOD is designed to work with any U.S. county that has publicly available ACS and LODES data, making it suitable for large-scale cross-city studies. In contrast, existing tools like LARGEST or SCENARIO NET lack this coverage.
- 2) **Realistic spatial and temporal detail.** MOVEOD combines detailed building footprints from OpenStreetMap

and Microsoft Building Footprints with departure time and travel time distributions from ACS Tables B08302 and B08303, respectively. The combination produces OD pairs that are both spatially precise and timestamped down to the minute, offering much higher resolution.

3) **Open and adaptable design.** Unlike many existing tools that rely on proprietary data and opaque processes, MOVEOD is fully transparent: all modeling assumptions are accessible in open-source code and configuration files. This allows researchers to tailor the framework to new countries, data sources, or policy scenarios.

III. PROBLEM STATEMENT AND DATA SOURCES

A. Problem Statement

Our objective is to infer a fine-grained joint distribution of commute data, specified at the level of individual buildings and minutes of the day. For our case, the origins are residences and destinations are workplaces.

Spatial sets Let \mathcal{G} be the set of all census-units (CUs) and \mathcal{B} be the sets of all buildings. For each $g \in \mathcal{G}$, we define its building set

$$B_g = \{b \in \mathcal{B} : G(b) = g\},$$

where $G : \mathcal{B} \rightarrow \mathcal{G}$ maps a building b to the census unit $G(b)$ that contains the building.

Origin and destination notation Each CU can serve both as an origin and a destination. Let $O \in \mathcal{G}$ represent the origin CUs and $D \in \mathcal{G}$ represent the destination CUs. When we need specific buildings, we write $b_o \in B_O, b_d \in B_D$, where b_o and b_d are sampled from the set of buildings in their respective census units.

Temporal distribution Each origin census unit (CU) $o \in \mathcal{G}$ has an associated set of departure time blocks defined by ACS, denoted as $\mathcal{T}_o = \{T_o^1, T_o^2, \dots, T_o^t\}$, where each $T_o^i = [\ell^i, u^i]$ represents a time interval in hours (e.g., $[0, 6]$ for “Before 6 AM”, $[6, 7]$ for “6–7 AM”, etc.).

We discretize the day into 1440 minutes indexed by $S \in \{0, 1, \dots, 1439\}$, with each S corresponding to $S/60$ real-time hours.

To assign a time block to each minute, we define a function: $T_o(S) = T_o^i$ if $\ell^i \leq \frac{S}{60} < u^i$. This mapping forms the bridge between fine-grained temporal resolution and the coarser ACS departure time distribution.

Each commuter’s trip The random vector describing a commuter’s trip is (B_O, B_D, S, E) , where

$B_O \in \mathcal{B}$	is the origin CU building,
$B_D \in \mathcal{B}$	is the destination CU building,
$S \in \{0, 1, \dots, 1439\}$	is the departure time from origin CU,
$E \in \{0, 1, \dots, 1439\}$	is the arrival time at destination CU.

A specific commuter is represented as (b_o, b_d, s, e) , and our goal is to estimate

$$P(B_O = b_o, B_D = b_d, S = s, E = e),$$

TABLE I: Data sources

Symbol	Type	Description
$\langle O, D \rangle$	LODES	Origin-destination flow data
$\langle O, T \rangle$	ACS B08302	Departure time by origin census unit
$\langle O, J \rangle$	ACS B08303	Travel time distribution by origin CU
\mathcal{B}	OSM/MSBF	Building footprints (residence/workplace)
\mathcal{V}	INRIX/OSM	Road speed data (hourly)

TABLE II: Key symbols

Input Variables		
Symbol	Type	Description
\mathcal{G}	Set	Census units (CUs)
\mathcal{B}	Set	Buildings
\mathcal{T}	Set	Departure time blocks
\mathcal{J}	Set	Travel time categories
\mathcal{M}	Set	Generated OD dataset
N	Constant	Total population size
Commuter Variables		
Symbol	Type	Description
B_O	Variable	Origin building location
B_D	Variable	Destination building location
S	Variable	Departure time (minutes)
E	Variable	Arrival time (minutes)

even though available public data provide only coarsened marginals such as $P(G(b_o) = g_o, G(b_d) = g_d)$ or $P(G(b_o) = g_o, T(S) = T_j)$.

B. Public Data Sources

Our framework relies exclusively on publicly available datasets to provide the spatial and temporal inputs needed for OD synthesis. Table I provides a summary of the data sources used. Below, we outline how we acquire and pre-process each dataset.

Census unit (CU) To obtain the census-unit geometries (\mathcal{G}), we download the U.S. Census Bureau’s TIGER/Line shapefiles for block groups (or other desired summary level) directly from the Census website. These open-source TIGER/Line files provide precise polygon boundaries for every block-group in the United States.

LODES We treat the LEHD Origin–Destination Employment Statistics (LODES) counts [40] as an empirical joint distribution over origin and destination CUs. For $(o, d) \in \mathcal{G} \times \mathcal{G} : \lambda_{o,d} = |\{\text{commuters with origin CU } o, \text{ destination CU } d\}|$ Then the estimated probability mass function for the CU–pair (O, D) , conditioning on the origin is

$$\hat{P}_{O,D}(D = d | O = o) = \frac{\lambda_{o,d}}{\sum_{d' \in \mathcal{G}} \lambda_{o,d'}}.$$

ACS Tables ACS tables provide statistically weighted estimates of commuting behavior at the census block-group level, including departure time distributions, mode of transport, and origin-destination flows, serving as ground-truth marginals for synthetic OD generation.

ACS Table B08302 (Departure Time Marginals) Let \mathcal{C}_{dep} be the weighted set of commuter records in ACS table B08302. Each record $c \in \mathcal{C}_{\text{dep}}$ includes $O_c \in \mathcal{G}$ and $T_c \in \mathcal{T}$, namely, its origin CU and its departure time block. For every

$o \in \mathcal{G}$ and $t \in \mathcal{T}$, define $\lambda_{o,t} = |\{c \in \mathcal{C}_{\text{dep}} : O_c = o, T_c = t\}|$. By construction, $\sum_{t \in \mathcal{T}} \lambda_{o,t} = N_o$, i.e., the total commuter count at origin o . We then set $\hat{P}(T = t | O = o) = \frac{\lambda_{o,t}}{N_o}$, treating $\hat{P}(T | O)$ as the ground-truth origin-time marginal. Since ACS is a population-weighted survey, these proportions accurately reflect how many people leave origin o in each departure time block t .

ACS Table B08303 (Travel-Time Marginals) Let \mathcal{C}_{tt} be the weighted set of travel time records in ACS B08303. The travel-time random variable is $\delta = E - S, \delta \in \mathbb{N}$ and let $\mathcal{J} = \{J_1, \dots, J_k\}$ be the ACS-defined travel-time intervals (bins), where each $J_j = [\ell_j^\delta, u_j^\delta], j = 1, \dots, n$ specifies a range of durations in minutes (e.g. $[0, 5)$, $[5, 10)$). For each origin CU $o \in \mathcal{G}$ and bin J_j , ACS B08303 reports a count $\lambda_{o,j} = |\{c \in \mathcal{C}_{\text{tt}} : O_c = o, \delta_c \in J_j\}|$, where $O_c \in \mathcal{G}$ is the origin CU and $\delta_c = E_c - S_c$ is the commute duration for record c . We normalize to obtain the empirical joint distribution $\hat{P}(J = j | O = o) = \frac{\lambda_{o,j}}{\sum_{j'} \lambda_{o,j'}}$. This $\hat{P}(J | O)$ serves as our estimate of the true CU conditional travel-time distribution.

Tiered building selection. Each building $b \in \mathcal{B}$ is assigned to its census unit $G(b) \in \mathcal{G}$. We start with two footprint sets: $\mathcal{B}_{\text{OSM}} = \{\text{OSM footprints with land-use tag } L(b)\}$, $\mathcal{B}_{\text{MS}} = \{\text{Microsoft building footprints}\}$. For each CU g , let

$$\begin{aligned}\mathcal{B}_{\text{OSM},g}^{\text{res}} &= \{b \in \mathcal{B}_{\text{OSM}} : G(b) = g, L(b) = \text{residential}\}, \\ \mathcal{B}_{\text{OSM},g}^{\text{com}} &= \{b \in \mathcal{B}_{\text{OSM}} : G(b) = g, L(b) = \text{commercial}\}, \\ \mathcal{B}_{\text{MSBF},g} &= \{b \in \mathcal{B}_{\text{MSBF}} : G(b) = g\}.\end{aligned}$$

We then define the candidate origin-building set \mathcal{B}_o and destination-building set \mathcal{B}_d by a three-tier rule:

$$\begin{aligned}\mathcal{B}_o &= \begin{cases} \mathcal{B}_{\text{OSM},o}^{\text{res}}, & \text{if } \mathcal{B}_{\text{OSM},o}^{\text{res}} \neq \emptyset, \\ \mathcal{B}_{\text{MSBF},o}, & \text{else if } \mathcal{B}_{\text{MSBF},o} \neq \emptyset, \\ \{\text{centroid}(o)\}, & \text{otherwise,} \end{cases} \\ \mathcal{B}_d &= \begin{cases} \mathcal{B}_{\text{OSM},d}^{\text{com}}, & \text{if } \mathcal{B}_{\text{OSM},d}^{\text{com}} \neq \emptyset, \\ \mathcal{B}_{\text{MSBF},d}, & \text{else if } \mathcal{B}_{\text{MSBF},d} \neq \emptyset, \\ \{\text{centroid}(d)\}, & \text{otherwise.} \end{cases}\end{aligned}$$

Thus, for a sampled origin CU o , we select an origin building $b_o \in \mathcal{B}_o$; and for a sampled destination CU d , we select $b_d \in \mathcal{B}_d$. This tiered approach ensures that we use tagged buildings when available, with a fallback to less-specific data otherwise.

Real road speeds. We assign each road segment $z \in \mathcal{Z}$ a speed $v \in \mathcal{V}$ in one of two ways:

- **OpenStreetMaps (OSM) defaults:** Provides the road network and each road segment's speed limit, or a standard average speed based on the type of road.
- **INRIX data:** Provides hourly road speeds using average measurements from roadside sensors. For each departure time block T , we use the mean road speed over all constituent hours to estimate travel durations in that period.

We use INRIX speed values for roads where INRIX data are available; for other roads, we use speed values based on OSM. This hybrid approach yields a granular travel-time profile $\tau_z(t)$

for road segment $z \in \mathcal{Z}$ at departure time block t that drives our realistic OD travel-time assignment. Table II provides an overview of the symbols used.

IV. METHODOLOGY

A. Adjusting LODES OD Flows with ACS distributions

ACS Table B08302 tells us how many commuters depart from each origin CU $o \in \mathcal{G}$ over the day (or per departure block), but it does not specify where they go. LODES, on the other hand, provides a full OD matrix $\lambda_{o,d}$ of workers traveling from origin CU o to destination CU d , yet its row totals $\sum_d \lambda_{o,d}$ rarely match the ACS commuter counts N_o .

We therefore adjust the number of commuters for each LODES origin-destination CU pair such that its sum equals the ACS distribution, keeping the proportion of commuters to each destination unchanged:

$$\alpha_o = \frac{T_o}{\sum_d \lambda_{o,d}}, \quad \tilde{\lambda}_{o,d} = \alpha_o \cdot \lambda_{o,d}.$$

Now $\sum_d \tilde{\lambda}_{o,d} = T_o$ for every origin o and the conditional destination distribution is preserved, as

$$\hat{P}(D = d | O = o) = \frac{\tilde{\lambda}_{o,d}}{\sum_{d' \in \mathcal{G}} \tilde{\lambda}_{o,d'}} = \frac{\lambda_{o,d}}{\sum_{d' \in \mathcal{G}} \lambda_{o,d'}}.$$

B. Bayesian Decomposition.

Our target is the full joint $P(O, D, S, E)$. By the chain rule, $P(O, D, S, E) = P(E | S, D, O) P(S | D, O) P(D | O) P(O)$. We simplify with a reasonable assumption that: Departure time S depends only on the origin: $P(S | D, O) = P(S | O)$. Thus $P(O, D, S, E) = P(E | S, D, O) P(S | O) P(D | O) P(O)$.

We estimate each factor as follows:

- $P(D | O)$ from LODES and tiered building choice.
- $P(O)$ from LODES and $P(S | O)$ from ACS B08302.
- $P(E | S, D, O)$ by fitting a travel-time distribution to ACS B08303 and road speed feeds.

Combining these steps yields a fully specified $P(O, D, S, E)$ that is consistent with all available public distributions, and can be sampled to produce building- and minute-level synthetic OD trips.

The data sources (Section III-B) give us four anchors:

- 1) Adjusted origin CU to destination CU counts $\tilde{\lambda}_{o,d}$ that already respect the ACS origin and departure time distributions.
- 2) Building location sets B_O and B_D represent the residential and commercial buildings, respectively, in every CU.
- 3) The conditional marginal distribution of departure time $\hat{P}(T = t | O = o)$.
- 4) The conditional marginal distribution of travel time $\hat{P}(J = j | O = o)$.

The methodology below turns these anchors into a minute-level, building-level OD data set $\mathcal{M} = \{(b_o, b_d, s, e)\}$ and then calibrates the synthetic travel-time distribution to ACS table B08303.

C. Spatial Sampling

Within each census unit, we assign origin and destination buildings uniformly to each of the $\tilde{\lambda}_{o,d}$ commute trips, prioritizing tagged buildings over untagged ones, as described earlier. For each CU, $g \in \mathcal{G}$, the set of buildings is

$$\mathcal{B}_g = \begin{cases} \mathcal{B}_{\text{OSM},g}^{\text{res}}, & \text{if } \mathcal{B}_{\text{OSM},g}^{\text{res}} \neq \emptyset, \\ \mathcal{B}_{\text{MSBF},g}, & \text{else if } \mathcal{B}_{\text{MSBF},g} \neq \emptyset, \\ \{\text{centroid}(g)\}, & \text{otherwise.} \end{cases}$$

For all origins in O and destinations in D ,

$$P(O = o, D = d) = \frac{\tilde{\lambda}_{o,d}}{N} \times \frac{1}{|B_O|} \times \frac{1}{|B_D|},$$

where $N = \sum_{o,d} \tilde{\lambda}_{o,d}$, and B_O, B_D are the sets of origin and destination buildings, respectively. The result is an OD sample that (i) matches ACS origin CU totals, (ii) inherits LODES destination splits, and (iii) resolves to individual buildings and departure-time blocks.

D. Departure-Time Assignment

Earlier, we defined the ACS departure time distribution as $\hat{P}(T = t | O = o)$. Because ACS is a population-weighted survey, we treat $\hat{P}(T | O)$ as the ground-truth for origins O and we choose the departure time block by sampling from the departure time marginal probability $s \sim \hat{P}(T = t | O = o)$. Given origin CU o and departure time t , we choose a specific minute uniformly inside the time bounds $[\ell_t, u_t]$ hours: $s \sim \text{Uniform}(\ell_t, u_t)$. Because the number of synthetic departures in each block was fixed to $T_o(t)$ during preprocessing, this step preserves the O and T distributions.

E. Travel-Time Estimation

Next, we find the arrival time at destination E . For each sampled tuple $(b_o, b_d, s) \in \mathcal{M}$ we compute:

- the route length $l_{o,d} = \text{graph-distance}(b_o, b_d)$,
- the shortest-path travel time $\tau_{o,d}(s) = \text{duration}(b_o, b_d | \text{depart } s)$,
- the reported speed $v_{o,d}(s) = \frac{l_{o,d}}{\tau_{o,d}(s)}$

These values are stored in the sets $\Omega = \{\tau_{o,d}(s)\}$, indexed by each $(b_o, b_d, s) \in \mathcal{M}$.

Based on travel time $\tau_{o,d}(s)$, we calculate the arrival time $e = s + \tau_{o,d}(s)$, and provide complete information $(b_o, b_d, s, e) \in \mathcal{M}$ for each commuter.

F. Initial OD Dataset

The three steps above yield a building and time-resolved OD dataset $\mathcal{M} = \{(b_o, b_d, s, e)\}$ that by construction satisfies ACS origin totals, LODES destination splits, and ACS departure-block distributions.

Algorithm 1: MOVEOD: Building-Level OD Generation

Input: $\tilde{\lambda}_{o,d}$ (adjusted OD counts with ACS marginals);
 B_O, B_D (building lookup tables);
 $\hat{P}(T = t | O = o)$ (departure marginals);
 $\hat{P}(J = j | O = o)$ (travel-time marginals)
Output: $\mathcal{M} = \{(b_o, b_d, s, e)\}$ initial OD dataset assignment

1 Step 1: Spatial Sampling:
2 foreach CU pair (o, d) and dep. block t **do**
3 for $i \leftarrow 1$ to $\tilde{\lambda}_{o,d}(t)$ **do**
4 $b_o \leftarrow \text{Unif}(B_O)$;
5 $b_d \leftarrow \text{Unif}(B_D)$;
6store provisional tuple (b_o, b_d) ;
7**end**
8 **end**

9 Step 2: Departure-Time Assignment:
10 foreach stored tuple (b_o, b_d, o, d, s) **do**
11draw block $t \sim \hat{P}(T = t | O = o)$;
12 $s \leftarrow \text{Unif}([\ell_t, u_t])$;
13add (b_o, b_d, s) to \mathcal{M} ;
14 **end**

15 Step 3: Raw Travel-Time Computation:
16 foreach $(b_o, b_d, s) \in \mathcal{M}$ **do**
17 $l_{o,d} \leftarrow \text{GraphDist}(b_o, b_d)$;
18 $\tau_{o,d}(s) \leftarrow \text{TravelTime}(b_o, b_d | s)$;
19 $e \leftarrow s + \tau_{o,d}(s)$;
20update record to (b_o, b_d, s, e) ;
21 **end**

22 Step 4: Mean-Speed Shift:
23 $\bar{\tau}^{\text{sim}} \leftarrow \frac{1}{|\mathcal{M}|} \sum \tau_{o,d}(s)$;
24 $\bar{\tau}^{\text{ACS}} \leftarrow \frac{\sum_o \sum_j k_j \hat{P}(J = j | O = o)}{\sum_o N_o}$;
25 $\psi \leftarrow \bar{\tau}^{\text{sim}} / \bar{\tau}^{\text{ACS}}$;
26 scale every road speed $v_e \leftarrow \psi v_e$;
27 **return** \mathcal{M}

G. Mean Speed Shift

At this stage, we have a complete dataset of origins, destinations, and departure times; however, the simulated mean travel times are typically shorter than those reported by the ACS. This is because self-reported survey times often overestimate actual travel due to rounding, inclusion of parking or waiting, and added buffer time [31], [37]. To correct for this bias without altering the OD or departure-time distributions, we apply a mean speed shift, resulting in a more realistic synthetic commuter dataset.

Let $N = |\mathcal{M}|$ be the total number of commuters. The mean travel time from the synthetic OD data is

$$\bar{\tau}^{\text{syn}} = \frac{1}{N} \sum_{\tau \in \Omega} \tau,$$

and the mean travel time from ACS (using travel time bin midpoints \bar{j}) is

$$\bar{\tau}^{\text{ACS}} = \frac{1}{\sum_o N_o} \sum_{o \in \mathcal{G}} \sum_{j \in \mathcal{J}} \bar{j} \hat{P}(J = j | O = o).$$

The mean speed shift is $\psi = \bar{\tau}^{\text{syn}} / \bar{\tau}^{\text{ACS}}$, and each road speed is modified to be $v'_e = \psi v_e$.

Algorithm 2: MOVEOD: Calibration

Input: $m_{o,d,t} \in \mathcal{M}$ (initial OD dataset) $\tilde{\lambda}_{o,d}$ (adjusted OD counts with ACS marginals);
 B_O, B_D (building lookup tables);
 $\hat{P}(T=t | O=o)$ (departure marginals);
 $\hat{P}(J=j | O=o)$ (travel-time marginals)
Output: $\mathcal{M} = \{(b_o, b_d, s, e)\}$ calibrated to all marginals

1 **Step 4: Mean-Speed Shift;**
2 $\bar{\tau}^{\text{syn}} \leftarrow \frac{1}{|\mathcal{M}|} \sum \tau_{o,d}(s);$
3 $\bar{\tau}^{\text{ACS}} \leftarrow \frac{\sum_o \sum_j k_j \hat{P}(J=j | O=o)}{\sum_o N_o};$
4 $\psi \leftarrow \bar{\tau}^{\text{syn}} / \bar{\tau}^{\text{ACS}};$
5 scale every road speed $v_e \leftarrow \psi v_e$;

6 **Step 5: Travel-Time Calibration (per origin o);**
7 **foreach** $o \in \mathcal{G}$ **do**
8 Extract raw commuter counts $m_{o,d,t}$ and targets: total count N_o , destination shares $\tilde{\lambda}_{o,d}$, departure time shares $\lambda_{o,t}$, and travel time shares $\lambda_{o,j}$;
9 Solve ILP to compute calibrated counts $a_{o,d,t}$ that:
 • exactly match N_o , $\tilde{\lambda}_{o,d}$, and $\lambda_{o,t}$
 • approximately match $\lambda_{o,j}$ (via slack variables)
 • stay close to $m_{o,d,t}$ (via penalized deviation)
 update \mathcal{M} using $a_{o,d,t}$ by resampling (b_o, b_d) and recomputing $e = s + \tau_{o,d}(s)$;
10 **end**
11 **return** \mathcal{M}

Algorithm 1 outlines the step-by-step process used to generate the initial OD dataset.

V. CALIBRATION

The goal is to calibrate the initial OD dataset \mathcal{M} so that the travel-time distribution matches the ACS travel time distribution while the origin-destination and origin-departure time distributions remain intact.

A. Inputs for a fixed origin CU $o \in \mathcal{G}$

- 1) $m_{o,d,t} \in \mathbb{Z}_{\geq 0}$: distribution of commuters from initial OD dataset, departing from origin o to destination d in departure time block $t \in \mathcal{T}$.
- 2) $N_o \in \mathbb{Z}_{\geq 0}$: total commuters whose home CU is o .
- 3) $\tilde{\lambda}_{o,d} \geq 0$, $\sum_{d \in \mathcal{G}} \tilde{\lambda}_{o,d} = 1$: Destination CU distribution of commuters from o who work in destination d (scaled LODES, Sec. IV).
- 4) $\lambda_{o,t} \geq 0$, $\sum_{t \in \mathcal{T}} \lambda_{o,t} = 1$: Departure time distribution of commuters from o that depart in block s (ACS B08302).
- 5) $\lambda_{o,j} \geq 0$, $\sum_{j \in \mathcal{J}} \lambda_{o,j} = 1$: travel-time share of commuters from o whose duration falls in ACS bin $j \in \mathcal{J}$ (ACS B08303).

B. Decision variables

- 1) $a_{o,d,t} \in \mathbb{Z}_{\geq 0}$ – calibrated number of commuters assigned to cell $(d, t) \in \mathcal{G} \times \mathcal{T}$.
- 2) $\epsilon_j^+, \epsilon_j^- \geq 0$ – slacks for travel-time bin $j \in \mathcal{J}$.
- 3) $\zeta_{o,d,t}^+, \zeta_{o,d,t}^- \geq 0$ – slacks measuring deviation from initial OD dataset $m_{o,d,t}$.

C. Integer linear program

Objective:

$$\min \alpha \sum_{j \in \mathcal{J}} (\epsilon_j^+ + \epsilon_j^-) + \beta \sum_{(d,t) \in \mathcal{G} \times \mathcal{T}} (\zeta_{o,d,t}^+ + \zeta_{o,d,t}^-)$$

Subject to:

- 1) $\sum_{(d,t) \in \mathcal{G} \times \mathcal{T}} a_{o,d,t} = N_o$
- 2) $\forall d \in \mathcal{G} : \sum_{t \in \mathcal{T}} a_{o,d,t} = N_o \cdot \tilde{\lambda}_{o,d}$
- 3) $\forall t \in \mathcal{T} : \sum_{d \in \mathcal{G}} a_{o,d,t} = N_o \cdot \lambda_{o,t}$
- 4) $\forall j \in \mathcal{J} : \sum_{(d,t) \in \mathcal{G} \times \mathcal{T}} a_{o,d,t} + \epsilon_j^- - \epsilon_j^+ = N_o \cdot \lambda_{o,j}$
- 5) $\forall (d,t) \in \mathcal{G} \times \mathcal{T} : a_{o,d,t} + \zeta_{o,d,t}^- - \zeta_{o,d,t}^+ = m_{o,d,t}$

Constraints (1)–(3) enforce the LODES and ACS distributions exactly. Constraint (4) matches the travel-time histogram up to the slacks $\epsilon_j^+, \epsilon_j^-$ (penalized by α). Constraint (5) keeps the new counts close to the initial OD dataset, to not completely violate the initial independence assumption in Section IV (penalized by β).

Algorithm 2 outlines the calibration process, detailing how we adjust the initial synthetic OD data to closely match observed marginal distributions from sources like LODES and ACS. This step ensures that the generated commuter flows accurately reflect real-world travel patterns and constraints.

The calibrated ODs $\{a_{o,d,t}\}$ feed back into $\mathcal{M} = \{(b_o, b_d, s, e)\}$ by resampling buildings inside each (o, d, t) origin and destination CU, and sampling a departure minute $s \in [\ell_t, u_t]$ within each departure time bin t and setting $e = s + \tau_{o,d}(s)$, where $\tau_{o,d}(s)$ is the road-network travel time. This produces a spatio-temporally resolved O, D, S, E dataset consistent with all empirical marginals.

VI. EXPERIMENTAL SETUP & RESULTS

We demonstrate that the pipeline behaves as intended by applying it to Davidson and Hamilton counties in Tennessee, U.S. With more than 336,000 commuters, Davidson County is the largest in Tennessee. We later use the Hamilton County OD dataset in multiple benchmarks. All the experiments were performed on a 32-core, 5.2 GHz, 32GB RAM Unix machine.

a) *Interactive interface:* MOVEOD uses a minimalist web interface where a user selects: state, county, range of dates to synthesize, the LODES release year, and an optional INRIX road speed feed.

All other inputs, such as the ACS tables, OSM, MSBF, and CU boundary files, are retrieved automatically. Pressing BEGIN returns ready-to-use calibrated OD tables, building metadata, and shapefiles within minutes.

For the α, β hyperparameters in the calibration step, we swept values from $[0, 1]$ at intervals of 0.1, for both. Experimentally, $\alpha = 1, \beta = 1$, provided the smallest gap with respect to the initial OD dataset $\sum_{(d,t)} (\zeta_{o,d,t}^+ + \zeta_{o,d,t}^-)$ and the ACS travel time distribution $\sum_j (\epsilon_j^+ + \epsilon_j^-)$.

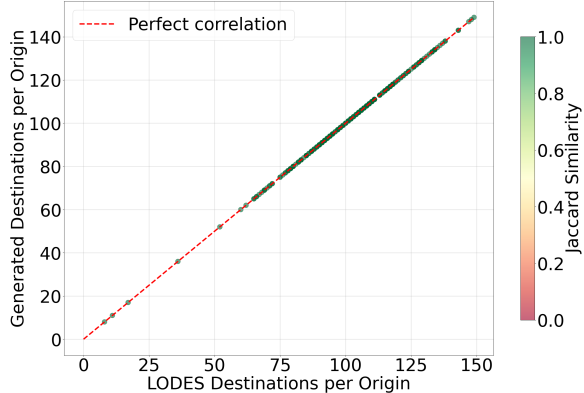


Fig. 1: MOVEOD preserves the conditional destination distribution for each origin census unit, ensuring that the synthetic workplace assignments match the empirical residence to work flow proportions reported in LODES.

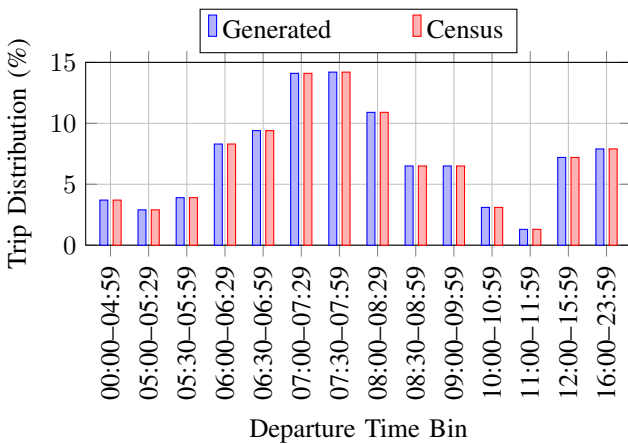


Fig. 2: MOVEOD calibrates the departure times for all origin census units to align with ACS departure times (B08302).

b) Validating the marginals: Figure 1 overlays the ACS modified LODES origin-departure distribution. The Jaccard similarity scores, $J(A, B) = |A \cap B|/|A \cup B|$, measuring the overlap between destination sets for each origin, exhibits a mean value of 1.0 for all origin CUs, as shown in Figure 2. This Jaccard similarity score indicates near-perfect structural preservation. Figure 2 overlays the ACS departure-time histogram with the synthetic departures; the two curves coincide, confirming that the block-level departure times are reproduced exactly. Figure 3 compares the travel-time distribution before and after calibration. Calibration shifts the simulated times toward the self-reported ACS curve, reducing the mean-absolute gap. These results validate that our calibration methodology successfully maintains the fundamental spatial and temporal structure of commuting patterns while adjusting the distributions to match observed travel time patterns.

Figure 3 compares the distribution of commute travel times across the initial commuter assignment (in blue), the calibrated commuter assignment (in red), and the ACS table B08303

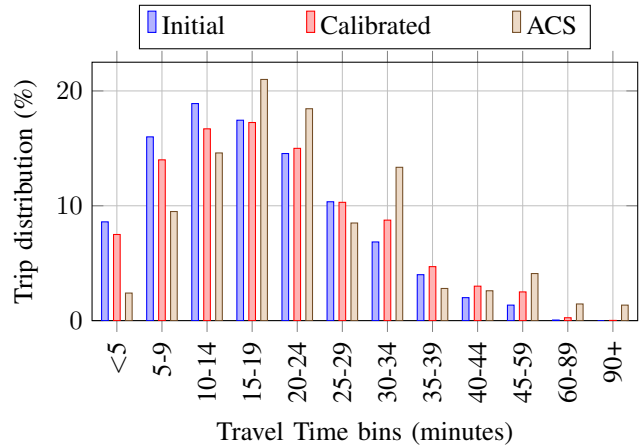


Fig. 3: Travel time distributions: initial commuter assignment (Initial), calibrated commuter assignment (Calibrated), and ACS travel time distribution (Table B08303).

distributions (in brown). The calibrated synthetic data are more closely aligned with the ACS distribution than the initial synthetic data, both in the left tail (up to 15 minutes) and the right tail of the distribution (20 to 90 minutes), and both the mode and overall shape are well preserved. However, the calibrated dataset slightly under-estimates the proportion of typical travel times (15-19 minutes) compared to ACS. The calibration process thus improves fidelity to observed census patterns, but some discrepancies remain around the mean of the distribution. Overall, the results indicate strong preservation of structure and successful calibration for most commuters.

Principally, the Hamilton County experiment shows that MOVEOD (i) honors all public marginals, (ii) exposes a tunable parameter to account for survey bias in travel times, and (iii) can be operated by non-experts through a browser. The potential origin and destination locations, \mathcal{B}_O and \mathcal{B}_D are shown in Fig. 4a and Fig. 4b, respectively. A sample of the calibrated commute trips for Hamilton County is visualized in Fig. 4c; note that visualizing all OD data ($>158,000$) makes the map illegible.

c) Time Complexity: The dominant cost is in generating and processing commuter trips, which scales linearly with the total number of trips M . Spatial sampling and departure-time assignment are both $O(M)$. Travel-time computation is $O(M \cdot \log Y)$, where $\log Y$ is the cost of finding paths per trip (using Dijkstra's algorithm with Y nodes). Adjusting mean speeds is $O(M + E)$, where Z is the number of road edges. Overall, the total runtime is $O(M \cdot \log Y + Z)$. The complete MOVEOD process takes 22 minutes for a county with 336,000 commuters, such as Davidson County, and 14 minutes for Hamilton County.

d) Space Complexity: Memory usage is $O(M)$ for storing all commuter assignments, $O(B)$ for building lookup tables where B is the number of buildings, $O(G \cdot (T + J))$ for ACS marginals (with G census units, T time blocks, J

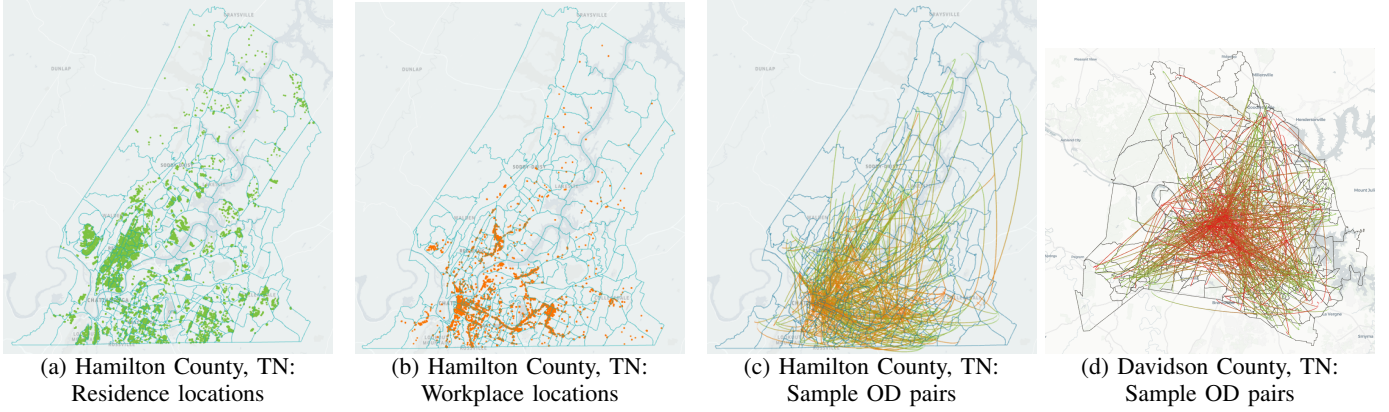


Fig. 4: MOVEOD commute data for Tennessee. (a) Residential building locations and (b) workplace locations in Hamilton County. (c) Sample of origin–destination (OD) commuter trips within Hamilton County, where each arc is shaded green at the origin and red at the destination. (d) Sample of OD trips for Davidson County, which has more than twice the number of commuters as Hamilton County.

travel-time bins), and $O(Z + E)$ for the road network. Thus, the total space complexity is $O(M + B + G \cdot (T + J) + Z + E)$.

VII. BENCHMARK EXPERIMENTS

In this section, we explain how we generate benchmark vehicle routing problem (VRP) instances from our calibrated OD data and evaluate different algorithms. The VRP [10], [39] is a classic optimization problem that asks how to route a fleet of vehicles as efficiently as possible to serve a set of locations. It's a motivating use case because it closely mirrors real-world challenges in public transit and ride-sharing.

A. Benchmark Vehicle Routing Problems

The calibrated commuter set $\mathcal{M} = \{(b_o, b_d, s, e)\}$ contains hundreds of thousands of trips, which usually exceeds computational limits of routing algorithms. Therefore, we draw a random sample $\tilde{\mathcal{M}}$ of size k without replacement:

Because every commuter in \mathcal{M} is equally likely to be chosen (probability $k/|\mathcal{M}|$), The expected number of sampled trips that originate in the census unit o is

$$\mathbb{E}[|\tilde{\mathcal{M}} \cap \mathcal{M}_o|] = \frac{k}{|\mathcal{M}|} |\mathcal{M}_o|,$$

which preserves (in expectation) the relative magnitudes of origin-specific flows while making the instance tractable.¹

VRP instance construction. Each sampled tuple $(b_o, b_d, s, e) \in \tilde{\mathcal{M}}$ is converted into a customer of a Vehicle Routing Problem (VRP).

- **Depots:** One or more operating centers per county; vehicles start and finish their routes at the depots. For our case, the depot is chosen to be the centroid of all the CUs in the dataset (for both train and test datasets).
- **Customer nodes:** Each commuter induces a pickup–delivery pair (b_o, b_d) where $b_o \in \mathcal{B}_O$ is the

¹If a deterministic size per origin is required, one may draw $k_o = \lfloor k |\mathcal{M}_o| / |\mathcal{M}| \rfloor$ trips from each \mathcal{M}_o ; we use the simpler global random sample without replacement in our experiments.

k -th commuter's home building and $b_d \in \mathcal{B}_D$ is that commuter's workplace building. Both locations are taken directly from the building footprints.

- **Demand:** Each request is for a single passenger.
- **Cost:** Edge cost c_{ij} is the great-circle distance between buildings i and j (or the corresponding driving distance/time if a road network is supplied).
- **Time windows:** The pickup node b_o inherits the departure time s .

The objective of the problem is to serve all demand while covering the least distance both for the vehicles and the passengers. This sampling strategy yields routing test beds that are both computationally manageable and statistically faithful to the complete, calibrated OD demand.

B. Benchmark VRP Algorithms

We apply a diverse selection of benchmark algorithms to the generated VRP instances, including classical heuristic, meta-heuristic, and deep reinforcement learning (DRL) approaches. All implementations are the authors' reference code, executed with default hyper-parameters unless noted otherwise.

Classical constructive heuristics:

- 1) **Insertion** [34] The canonical cheapest insertion algorithm constructs vehicle routes by repeatedly inserting a customer whose marginal cost is minimal.
- 2) **Clarke–Wright** [33] A vehicle routing heuristic that starts with individual routes for each customer and iteratively merges pairs of routes. At each step, it selects the merge that maximizes the travel-cost savings.

Meta-heuristics:

- 1) **Simulated Annealing** [6] A single-tour search that accepts uphill moves with a probability governed by a decaying temperature schedule.
- 2) **Genetic Algorithm** [3] Population-based evolutionary search with order-crossover and inversion mutation.

TABLE III: CPDP Algorithm Performance (30 Vehicles with 5-Passenger Capacity)

Algorithm	VMT \downarrow	PMT \downarrow	VMT/PMT \downarrow	Empty \downarrow	Coverage \uparrow	Vehicle Utilization \uparrow	Routes \uparrow
LKH-3	2,255.16	1,455.74	1.55	40.9	100	100	30
Clarke–Wright Savings	2,622.84	1,455.74	1.80	49.9	100	100	30
Large Neighborhood Search	2,960.06	1,455.74	2.03	56.2	100	67	20
Genetic Algorithm	3,032.40	1,455.74	2.08	52.0	100	67	20
Simulated Annealing	3,239.05	1,455.74	2.23	55.1	100	100	30
Insertion Heuristic	3,281.13	1,455.74	2.25	55.6	100	67	20
Ant Colony Optimization	3,281.13	1,455.74	2.25	55.6	100	67	20
POMO	3,296.79	1,455.74	2.26	55.8	100	67	20
Attention Model	3,302.41	1,455.74	2.27	55.9	100	83	25

Arrows indicate performance direction: \downarrow means lower is better, \uparrow means higher is better. VMT – Vehicle Miles Traveled; PMT – Passenger Miles Traveled; Empty – percentage of distance traveled without passengers; Coverage – percentage of passengers served; Vehicle Utilization – percentage of available vehicles used; Routes – number of vehicle routes.

- 3) **Ant Colony Optimization** [35] A constructive meta-heuristic in which artificial “ants” deposit pheromone on promising edges, reinforcing good routes over time.
- 4) **Large Neighborhood Search** [9] Repeatedly destroys and repairs parts of a solution; here we use the classical Shaw destroy and regret-2 repair operators.

Exact / heuristic hybrid:

- 1) **LKH-3** [14] Helsgaun’s state-of-the-art Lin–Kernighan implementation which combines variable-opt moves, 1-tree lower bounds and potent kick-starts.

Deep-RL policies:

- 1) **Attention:** Kool et al. [21] propose an attention-based model trained with REINFORCE for learning heuristics to solve combinatorial optimization problems, specifically routing problems like the Traveling Salesman Problem and Vehicle Routing Problem.
- 2) **POMO:** Policy Optimization with Multiple Optima algorithm [22] is a deep reinforcement learning approach designed to address instability in policy gradient methods, particularly when applied to combinatorial optimization problems like the Vehicle Routing Problem.

C. Validation

To validate the operational utility of the OD data generated by MOVEOD, we simulate routing scenarios using VRP algorithms. The VRP problem we solve involves transporting a unit demand (commuter) from a known origin to a known destination, under vehicle capacity and a pickup time constraints. This formulation directly maps to commuter mobility, with each vehicle representing a shared transport vehicle, such as a shuttle or van.

We construct a validation benchmark by selecting $k = 100$ commuter trips from our calibrated OD data in Hamilton County, Tennessee to obtain $\tilde{\mathcal{M}}$. This sample size is chosen to provide a good balance between computational tractability and statistical reliability: it is large enough to capture meaningful trip variability, yet small enough to keep the computational cost of repeated routing experiments manageable. These are drawn exclusively from early-morning departures (between 12:00am and 4:59am), which serves as a representative subset of the dataset for benchmarking purposes. Each sampled trip

(b_o, b_d, s, e) defines a pickup–delivery pair with a unit demand, as described in Section VII-A.

For every OD instance we feed the same distance matrix, vehicle capacity and depot location to each algorithm, cap CPU time at 5 min, and record the best feasible solution cost.

Since some algorithms (notably Attention, POMO) require offline training, we partition the commuter data into disjoint training and testing sets. The split is based on geographic origin zones. To create the test set, we randomly designated a contiguous 20% of the total CUs as the test region. From these origins, 100 trips were sampled. All other CUs constitute the training region. This ensures a realistic generalization test as learning-based methods must route trips in areas not seen during training.

Each algorithm receives the same inputs: the coordinates of all buildings, cost matrix (shortest path travel times), vehicle capacity of 5 passengers, and a fleet of 30 identical vehicles. Algorithms are evaluated on their performance over the *test* set. All results are summarized in Table III.

Our experiments show that MOVEOD generated commuter flows yield tractable, solvable CPDP instances. Solutions are consistent across algorithms, with heuristics like LKH-3 and Clarke–Wright producing near-optimal routes, and learning-based methods generalizing reasonably well. This validates both the fidelity of MOVEOD’s synthetic demand and its usability in routing-centric transportation studies.

VIII. DISCUSSION AND CONCLUSIONS

MOVEOD delivers building- and minute-level commuter flows by fusing LODES OD distribution, ACS departure-time and travel-time distributions, and building footprints from OpenStreetMap and Microsoft Building Footprints. Unlike prior efforts that consider either where or when people commute, MOVEOD matches both spatial and temporal dimensions to ground-truth marginal distributions, yet remains fast enough to apply to any U.S. county.

Data access. A browser-based tool available to download at https://anonymous.4open.science/r/move_od-ED66/ lets users choose a state, county, date, and optional spatial or temporal filters, then generates calibrated OD data in minutes.

Typical applications. OD data show where people can commute for their work, which is one of the primary reasons for

travel and produces peak traffic conditions. OD data can be used for applications such as (i) predicting traffic flows of a county, (ii) public transit design (iii) and efficient road network design.

Moreover, the data generation framework is designed to be flexible: it can ingest any macro-level movement dataset (e.g., mobile phone traces, transit smart card records, or traffic sensor counts) and enhance spatial resolution to building-level origins and destinations. If temporal distributions (e.g., departure times, travel durations) are available, the process further refines the OD dataset with time-aware commuter assignments. This adaptability allows integration with diverse data sources, such as crowd-sourced GPS trajectories or emerging Internet of Things (IoT) mobility streams.

Limitations and outlook. MOVEOD generates OD data only for commute trips, assuming a typical weekday. Future work will add non-commute trips, consider weather and seasonal effects, and ingest real-time traffic speed data to capture day-specific congestion.

Key takeaway. By transforming public data into high-resolution, privacy-preserving OD flows, MOVEOD lowers the barrier to rigorous, reproducible experimentation in transportation planning and operations research.

REFERENCES

- [1] J. M. Abowd, J. Haltiwanger, and J. Lane. Integrated longitudinal employer-employee data for the united states. *American Economic Review*, 94(2):224–229, 2004.
- [2] J. Alonso-Mora, S. Samaranayake, A. Wallar, E. Frazzoli, and D. Rus. On-demand high-capacity ride-sharing via dynamic trip-vehicle assignment. *Proceedings of the National Academy of Sciences*, 114(3):462–467, 2017.
- [3] B. M. Baker and M. Ayelew. A genetic algorithm for the vehicle routing problem. *Computers & Operations Research*, 30(5):787–800, 2003.
- [4] E. Cipriani, S. Gori, and M. Petrelli. Transit network design: A procedure and an application to a large urban area. *Transportation Research Part C: Emerging Technologies*, 20(1):3–14, 2012.
- [5] F. Crawford, D. P. Watling, and R. D. Connors. Identifying road user classes based on repeated trip behaviour using bluetooth data. *Transportation Research Part A: Policy and Practice*, 113:55–74, 2018.
- [6] Z. J. Czech and P. Czarnas. Parallel simulated annealing for the vehicle routing problem with time windows. In *10th Euromicro Workshop on Parallel, Distributed and Network-based Processing*, pages 376–383. IEEE, 2002.
- [7] F. F. Dias, P. S. Lavieri, T. Kim, C. R. Bhat, and R. M. Pendyala. Fusing multiple sources of data to understand ride-hailing use. *Transportation Research Record*, 2673(6):214–224, 2019.
- [8] W. Du, J. Ye, J. Gu, J. Li, H. Wei, and G. Wang. Safelight: A reinforcement learning method toward collision-free traffic signal control. In *AAAI Conference on Artificial Intelligence*, volume 37, pages 14801–14810, 2023.
- [9] D. Dumez, F. Lehuédé, and O. Péton. A large neighborhood search approach to the vehicle routing problem with delivery options. *Transportation Research Part B: Methodological*, 144:103–132, 2021.
- [10] B. Eksioglu, A. V. Vural, and A. Reisman. The vehicle routing problem: A taxonomic review. *Computers & Industrial Engineering*, 57(4):1472–1483, 2009.
- [11] N. Ferreira, J. Poco, H. T. Vo, J. Freire, and C. T. Silva. Visual exploration of big spatio-temporal urban data: A study of new york city taxi trips. *IEEE Transactions on Visualization and Computer Graphics*, 19(12):2149–2158, 2013.
- [12] V. Guihaire and J.-K. Hao. Transit network design and scheduling: A global review. *Transportation Research Part A: Policy and Practice*, 42(10):1251–1273, 2008.
- [13] D. Guo, X. Zhu, H. Jin, P. Gao, and C. Andris. Discovering spatial patterns in origin-destination mobility data. *Transactions in GIS*, 16(3):411–429, 2012.
- [14] K. Helsgaun. An extension of the Lin-Kernighan-Helsgaun TSP solver for constrained traveling salesman and vehicle routing problems. *Roskilde: Roskilde University*, 12:966–980, 2017.
- [15] M. P. Heris, N. L. Foks, K. J. Bagstad, A. Troy, and Z. H. Ancona. A rasterized building footprint dataset for the united states. *Scientific Data*, 7(1):207, 2020.
- [16] S. Huang, C. Zhang, J. Zhao, and Y. Han. Traffic origin–destination flow prediction considering individual travel frequency: A classification-based approach. *Journal of Transportation Engineering, Part A: Systems*, 151(2):04024106, 2025.
- [17] O. Irimia, M. Panaite-Lehadus, C. Tomozei, E. Mosnegutu, and G. Przydatek. Origin-destination traffic survey—case study: Data analyse for bacau municipality. *Sustainability*, 15(6):4975, 2023.
- [18] R. Jiang, D. Yin, Z. Wang, Y. Wang, J. Deng, H. Liu, Z. Cai, J. Deng, X. Song, and R. Shibasaki. Dl-traff: Survey and benchmark of deep learning models for urban traffic prediction. In *30th ACM International Conference on Information & Knowledge Management (CIKM)*, pages 4515–4525, 2021.
- [19] T. Kashiyama, Y. Pang, and Y. Sekimoto. Open pflow: Creation and evaluation of an open dataset for typical people mass movement in urban areas. *Transportation Research Part C: Emerging Technologies*, 85:249–267, 2017.
- [20] R. Kitchin. *The data revolution: Big data, open data, data infrastructures and their consequences*. Sage, 2014.
- [21] W. Kool, H. van Hoof, and M. Welling. Attention, learn to solve routing problems! In *7th International Conference on Learning Representations (ICLR)*, 2019.
- [22] Y.-D. Kwon, J. Choo, B. Kim, I. Yoon, Y. Gwon, and S. Min. Pomo: Policy optimization with multiple optima for reinforcement learning. *Advances in Neural Information Processing Systems*, 33, 2020.
- [23] Q. Li, Z. M. Peng, L. Feng, Z. Liu, C. Duan, W. Mo, and B. Zhou. ScenarioNet: Open-source platform for large-scale traffic scenario simulation and modeling. *Advances in Neural Information Processing Systems*, 36:3894–3920, 2023.
- [24] S. Li, Z. Yan, and C. Wu. Learning to delegate for large-scale vehicle routing. *Advances in Neural Information Processing Systems (NeurIPS)*, 34:26198–26211, 2021.
- [25] Y. Li, R. Yu, C. Shahabi, and Y. Liu. Diffusion convolutional recurrent neural network: Data-driven traffic forecasting. *arXiv preprint arXiv:1707.01926*, 2017.
- [26] X. Liu, Y. Xia, Y. Liang, J. Hu, Y. Wang, L. Bai, C. Huang, Z. Liu, B. Hooi, and R. Zimmermann. Largest: A benchmark dataset for large-scale traffic forecasting. In *Advances in Neural Information Processing Systems*, 2023.
- [27] S. Liyanage and H. Dia. An agent-based simulation approach for evaluating the performance of on-demand bus services. *Sustainability*, 12(10):4117, 2020.
- [28] M. Mohammed and J. Oke. Origin-destination inference in public transportation systems: A comprehensive review. *International Journal of Transportation Science and Technology*, 12(1):315–328, 2023.
- [29] P. Mooney, M. Minghini, et al. A review of openstreetmap data. *Mapping and the citizen sensor*, pages 37–59, 2017.
- [30] National Research Council and National Academies of Sciences, Engineering, and Medicine. *Using the American Community Survey: Benefits and Challenges*. The National Academies Press, Washington, DC, 2007.
- [31] S. Peer, J. Knockaert, P. Koster, and E. T. Verhoef. Over-reporting vs. overreacting: Commuters’ perceptions of travel times. *Transportation Research Part A: Policy and Practice*, 69:476–494, 2014.
- [32] D. Perlman, K. Tufte, L. Flint, and T. Reel. Emerging data science for transit: Market scan and feasibility analysis. Technical Report FTA Report No. 0218, U.S. Department of Transportation, Federal Transit Administration, Washington, D.C., June 2022. Prepared by the John A. Volpe National Transportation Systems Center.
- [33] T. Pichpipul and R. Kawtummachai. A heuristic approach based on clarke-wright algorithm for open vehicle routing problem. *Scientific World Journal*, 2013(1):874349, 2013.
- [34] M. Randall, A. Kheiri, and A. N. Letchford. Insertion heuristics for a class of dynamic vehicle routing problems, 2022.
- [35] A. E. Rizzoli, R. Montemanni, E. Lucibello, and L. M. Gambardella. Ant colony optimization for real-world vehicle routing problems: from theory to applications. *Swarm Intelligence*, 1:135–151, 2007.

- [36] R. Sen, T. Tran, S. Khaleghian, P. Pugliese, M. Sartipi, H. Neema, and A. Dubey. Bte-sim: Fast simulation environment for public transportation. In *2022 IEEE International Conference on Big Data (Big Data)*, pages 2886–2894, 2022.
- [37] P. R. Stopher and S. P. Greaves. Household travel surveys: Where are we going? *Transportation Research Part A: Policy and Practice*, 41(5):367–381, 2007.
- [38] P. Thakuriah, N. Y. Tilahun, and M. Zellner. *Introduction to seeing cities through big data: Research, methods and applications in urban informatics*. Springer, 2017.
- [39] P. Toth and D. Vigo. *Vehicle routing: problems, methods, and applications*. SIAM, 2014.
- [40] United States Census Bureau. Longitudinal Employer-Household Dynamics - Origin-Destination Employment Statistics, 2017.
- [41] S. Uppoor, O. Trullols-Cruces, M. Fiore, and J. M. Barcelo-Ordinas. Generation and analysis of a large-scale urban vehicular mobility dataset. *IEEE Transactions on Mobile Computing*, 13(5):1061–1075, 2013.
- [42] W. Wang, W. Jiang, B. Zhang, Q. Zhu, and C. Liao. A real network environment dataset for traffic analysis. *Scientific Data*, 12(1):1–12, 2025.
- [43] B. Xu, Y. Wang, Z. Wang, H. Jia, and Z. Lu. Hierarchically and cooperatively learning traffic signal control. In *AAAI Conference on Artificial Intelligence*, volume 35, pages 669–677, 2021.
- [44] X. Xu, Z. Zheng, Z. Hu, K. Feng, and W. Ma. A unified dataset for the city-scale traffic assignment model in 20 us cities. *Scientific Data*, 11(1):325, 2024.